

# Dynamic-Dark SLAM: RGB-Thermal Cooperative Robot Vision Strategy for Multi-Person Tracking in Both Well-Lit and Low-Light Scenes

Tatsuro Sakai, Kanji Tanaka, Jonathan Tay Yu Liang, Muhammad Adil Luqman, Daiki Iwata  
University of Fukui  
3-9-1, bunkyo, fukui, fukui, Japan  
tnkknj@u-fukui.ac.jp

## Abstract

In robot vision, thermal cameras have significant potential for recognizing humans even in complete darkness. However, their application to multi-person tracking (MPT) has lagged due to data scarcity and difficulties in individual identification. In this study, we propose a cooperative MPT system that utilizes co-located RGB and thermal cameras, using pseudo-annotations (bounding boxes + person IDs) to train RGB and T trackers. Evaluation experiments demonstrate that the T tracker achieves remarkable performance in both bright and dark scenes. Furthermore, results suggest that a tracker-switching approach using a binary brightness classifier is more suitable than a tracker-fusion approach for information integration. This study marks a crucial first step toward “Dynamic-Dark SLAM,” enabling effective recognition, understanding, and reconstruction of individuals, occluding objects, and traversable areas in dynamic environments, both bright and dark.

## 1 Introduction

Thermal cameras (T-cameras) hold great potential for person detection and tracking in dark or low-light scenes, representing a promising new application in robot vision. Despite the increasing demand for advanced vision systems that consider privacy, such as those used in nighttime festivals and security patrols, T-vision remains underutilized, particularly in its application to multi-person tracking (MPT). MPT is a crucial technology in robot vision and is employed in various applications, including user tracking [1], patrolling [2], dynamic SLAM [3], structure-from-occlusion [4], and traversability analysis [5]. Research on MPT has primarily been based on RGB vision [6], while challenges specific to T-vision remain largely unaddressed.

One of the major obstacles in applying T-vision to MPT is the lack of annotated datasets (bounding boxes + person IDs), which makes supervised training of a T-tracker infeasible. These datasets are typically represented as time-series pairs of bounding boxes and person IDs. However, most existing datasets focus on



Figure 1. Crowded scenes and RGB-T cooperative vision.

RGB vision, and thermal image datasets are not yet well established. Furthermore, person ID identification in thermal images is difficult and requires high-cost annotation efforts to achieve accuracy. As a result, applying tracking techniques designed for RGB vision to T-vision leads to a decrease in performance (Fig. 2). Notably, the patterns in thermal images heavily depend on factors such as clothing, making them more complex than traditional RGB image patterns. Due to this dependency, generalizing thermal image datasets to arbitrary environments is difficult, necessitating the development of T-trackers that do not rely on annotated datasets.

In this study, we propose a novel cooperative MPT system that utilizes an RGB camera and a thermal (T) camera placed in the same pose, enabling effective tracking in both bright and dark conditions. The key idea is to train a T-tracker using knowledge transfer from an RGB-tracker in bright conditions. Among all possible combinations of (1) two scene types (Bright/Dark), (2) two modality types (RGB/T), (3) three tracker types (RGB/T/RGBT tracker), we exclude those that are clearly ineffective or redundant, leaving four viable combinations, as discussed in Section 4, which we then evaluate experimentally. The results demonstrate that the T-tracker achieves remarkable performance in both bright and dark scenes. Furthermore, our findings suggest that a tracker-switching approach using a binary brightness classifier is more suitable than a tracker-fusion approach for integrating the two trackers.



Figure 2. Output of the RGB tracker for the RGB image (left) and the T image (right).

This study builds on previous research on teacher-student knowledge transfer [7], multi-person tracking under occlusion [8], and the recognition, understanding, and reconstruction of people, occlusions, and traversable areas [9], effectively integrating thermal SLAM [10] and dynamic SLAM [3]. This marks a crucial first step toward “Dynamic-Dark SLAM,” enabling the effective recognition, understanding, and reconstruction of individuals, occluding objects, and traversable areas in both bright and dark dynamic environments.

## 2 Related Work

This study is related to several areas of research in robotic vision. In the field of robotics, research on multi-person tracking (MPT) has progressed using laser-based [11] and vision-based [12] methods, with the study of SLAM considering interactions between dynamic and static objects [3] being the most relevant to our work. However, most existing vision-based methods focus on RGB vision, leaving challenges specific to thermal (T) vision largely unresolved.

In the field of computer vision, studies on multi-sensor information fusion [13], such as RGB-LiDAR fusion, as well as research on teacher-student knowledge transfer [14], have been conducted. However, many of these studies rely on predefined cooperative schemes [15] where the teacher and student sensors are used complementarily at the same time, with little exploration of diverse cooperative strategies.

RGB-T fusion tracking has been studied in both non-deep approaches [16, 17, 18, 19] and deep approaches, including adaptive fusion [20], sparse fusion representation [21], cross-modal ranking [22], and graph models [23], as well as benchmark studies [24]. The approach of applying an RGB tracker [25] to the

RGB-T tracking problem was explored in [26]. Our approach is based on the state-of-the-art [ByteTrack] tracker and differs in that it handles Dark scenes, where RGB trackers completely fail.

## 3 RGB-T Cooperative MPT

### 3.1 Formulation of MPT

MPT is formulated as a problem where a tracker  $f$  takes an image sequence  $x_{1:T}$  as input and outputs a sequence of tracking results  $y_{1:T}$ . Here,  $x_{1:T} = (x_1, \dots, x_T)$  represents the sequence of camera images, where  $x_t$  denotes the image at time  $t$ . The tracking result is represented as  $y_t = \{y_t[i]\}_{i=1}^{I_t}$ , where  $I_t$  is the number of bounding boxes detected in the image  $x_t$  and each  $y_t[i]$  consists of  $(y_t^{\text{ID}}[i], y_t^{\text{BB}}[i], y_t^{\text{SCORE}}[i])$ . Specifically,  $y_t^{\text{ID}}[i]$  is the predicted ID of the person in the  $i$ -th bounding box,  $y_t^{\text{BB}}[i]$  represents the predicted location and size of the  $i$ -th bounding box, and  $y_t^{\text{SCORE}}[i]$  indicates the confidence score.

Given an annotated image sequence  $(x_{1:T}, y_{1:T})$ , the tracker is trained as follows:

$$\theta = \arg \min_{\theta} \mathcal{L}(f_{\theta}(x_{1:T}), y_{1:T}) \quad (1)$$

where  $\mathcal{L}$  represents the loss function that represents the error between the predicted results and the annotations.

### 3.2 ByteTrack

In this study, we propose using ByteTrack[27] as the baseline tracker, which separates detection from tracking and remains robust even under temporary full or partial occlusion. Many existing trackers discard detection results with scores below a threshold, whereas ByteTrack adopts a simple and general approach that utilizes low-score objects. Its core module consists of an object detector that outputs bounding boxes, scores, and classes for each frame, as well as a Byte module that associates tracked object IDs with detection results. ByteTrack employs a Kalman filter to predict the position of objects in frame  $t$  based on tracking information up to frame  $t - 1$ . Then, it associates predicted bounding boxes with actual detections in frame  $t$  based on Intersection over Union (IoU), matching the pairs with the highest IoU and selecting them based on a threshold.

This simple yet effective two-stage IoU matching method enables stable and fast tracking. In practice, ByteTrack demonstrated superior performance in our study. In addition to the main experiments, we conducted a comparative evaluation of three state-of-the-art trackers: OC-SORT [28], StrongSORT [29], and ByteTrack [27]. The RGB image sequence captured in a well-lit scene was used for this comparison because of the availability of high-quality ground-truth for such

sequences. The results showed that ByteTrack significantly outperformed OC-SORT and slightly more stable than StrongSORT.

The baseline tracker ByteTrack was trained as follows:

$$\theta^{\text{RGB}} = \arg \min_{\theta} \mathcal{L}^{\text{ByteTrack}}(f_{\theta}(x_{1:T}^{\text{RGB}}), y_{1:T}) \quad (2)$$

where  $\mathcal{L}^{\text{ByteTrack}}$  represents the loss function used in ByteTrack. The training set  $(x_{1:T}^{\text{RGB}}, y_{1:T})$  consists of five RGB image datasets: MOT17[30], MOT20[31], CrowdHuman[32], CityPersons[33], and ETHZ[34]. These datasets encompass various environments and scenarios, including urban settings, high-density crowds, occlusion scenarios, diverse weather conditions, and long-range pedestrian tracking, enhancing the model’s adaptability.

### 3.3 Cooperative Strategy

An RGB camera and a thermal (T) camera were placed at the same position and synchronized. By positioning the lenses of both cameras as closely as possible, we minimized the misalignment of the fields of view, reducing coordinate errors between the RGB and thermal images. Additionally, temporal discrepancies and resolution differences were corrected after capturing the data to precisely align the coordinates between the RGB and thermal images.

The input image at time  $t$  is defined as  $x_t = (x_t^{\text{RGB}}, x_t^{\text{T}})$ , where  $x_t^{\text{RGB}}$  represents the RGB image, and  $x_t^{\text{T}}$  represents the thermal image at time  $t$ .

The optimal coordinate transformation between the two camera coordinate systems may vary slightly depending on the environment. For instance, in a crowded environment such as that shown in Figure 2, pedestrians move while avoiding obstacles, leading to motion trajectories constrained by the obstacles. Therefore, it is possible to optimize the coordinate transformation based on pedestrian movement trajectories. In this study, a small set of image pairs of the same pedestrians observed from different cameras was used as training data to adjust the coordinate transformation parameters, minimizing transformation errors. Since the experimental environment ensured that both cameras captured the same plane or had minimal parallax, we modeled the relationship between the cameras using a homography transformation.

The experiments were conducted in an indoor environment with obstacles such as desks and chairs. Furthermore, we evaluated the multi-person tracking performance in a scene with four pedestrians.

In the experiment, an iPhone 15 was used as the RGB camera, while a FLIR One Pro was used as the thermal camera. The iPhone 15 captured images at a resolution of  $1920 \times 1080$  at 30 fps, while the FLIR One Pro captured images at a resolution of  $160 \times 120$  at 8.7 fps. To clearly visualize the temperature distribution,



Figure 3. Improved tracking results from the proposed method.

we used the “grayscale mode” to enhance the visibility of the target objects.

Using this synchronized dataset, tracking results (bounding boxes, person IDs, confidence scores) were obtained from the teacher model and used as pseudo-labels for thermal images.

$$\bar{y}_t = f_{\theta^{\text{RGB}}}(x_t^{\text{RGB}}) \quad (3)$$

The student model adapted to thermal images by minimizing a loss function considering both positional and classification errors between its predictions and the teacher model’s tracking results.

$$\theta^{\text{T}} = \arg \min_{\theta} \mathcal{L}^{\text{ByteTrack}}(f_{\theta}(x_{1:T}^{\text{T}}), \bar{y}_{1:T}) \quad (4)$$

Furthermore, a fusion model was introduced to complement the characteristics of both the teacher and student models.

$$\hat{y}_t = f_{\theta^{\text{RGB}\theta^{\text{T}}}}(x_t^{\text{RGB}}, x_t^{\text{T}}) \quad (5)$$

where  $f_{\theta^{\text{RGB}\theta^{\text{T}}}}$  represents the fusion function integrating both modalities. This fusion model integrates the tracking results of the RGB teacher model and the T student model, selecting the result with the higher confidence score in each frame to achieve robust tracking. For each  $i$  ( $i \in [1, I^t]$ ),  $y_t[i] = f^{\text{T}}(x_t^{\text{T}})$ ,  $\tilde{y}_t[j] = f^{\text{RGB}}(x_t^{\text{RGB}})$ , and for the corresponding pair  $j$  ( $j \in [1, I^t]$ ) satisfying  $y_t^{\text{ID}}[i] = \tilde{y}_t^{\text{ID}}[j]$ , the final fusion result is determined as follows:

$$\hat{y}_t[i] = \begin{cases} y_t[i] & \text{if } y_t^{\text{SCORE}}[i] > \tilde{y}_t^{\text{SCORE}}[j], \\ \tilde{y}_t[j] & \text{otherwise.} \end{cases} \quad (6)$$

## 4 Evaluation Experiment

The objective of this experiment is to evaluate the performance of RGB-T cooperative vision and identify

the optimal cooperation mode. The acquisition times of input images,  $\text{Full}=\{t\}_{t=1}^T$ , are divided into bright scene times and dark scene times, which are denoted as Bright and Dark, respectively ( $\text{Bright}\cup\text{Dark}=\text{Full}$ ,  $\text{Bright}\cap\text{Dark}=\emptyset$ ). Among all possible combinations of the two scene types (Bright/Dark), two modalities (RGB/T), and three trackers ( $f_{\theta_{\text{RGB}}}/f_{\theta_{\text{T}}}/f_{\theta_{\text{RGB}\theta_{\text{T}}}}$ ), meaningless and redundant combinations are excluded based on the following knowledge: (1) No tracker recognized RGB images in dark scenes<sup>1</sup> (2) T images were hardly affected by scene brightness<sup>2</sup>. As a result, the following four combinations remain:  $f_{\theta_{\text{RGB}}}(x_{\text{Full}}^{\text{T}})$ ,  $f_{\theta_{\text{T}}}(x_{\text{Full}}^{\text{T}})$ ,  $f_{\theta_{\text{RGB}}}(x_{\text{Bright}}^{\text{RGB}})+f_{\theta_{\text{T}}}(x_{\text{Dark}}^{\text{T}})$ , and  $f_{\theta_{\text{RGB}}}(x_{\text{Bright}}^{\text{RGB}})+f_{\theta_{\text{RGB}\theta_{\text{T}}}}(x_{\text{Dark}}^{\text{T}})$ .

This dataset consists of a training sequence of 8,970 synchronized RGB thermal image pairs, and three image sequences obtained from both RGB and thermal cameras in the Bright scene, containing 1,081 frames, 1,049 frames, and 1,010 frames, respectively, and a single image sequence from both RGB and thermal cameras in the Dark scene, containing 666 frames. For performance comparison, the ground truth data is manually annotated with bounding boxes and person IDs.

Each tracking method is evaluated using Multiple Object Tracking Accuracy (MOTA) and ID F1 score (IDF1) to assess tracking performance, along with False Positive (FP), True Positive (TP), and False Negative (FN) to evaluate false detections [35]. ID Switches (IDSW) and Higher Order Tracking Accuracy (HOTA) measure trajectory reconstruction, with HOTA providing a global tracking assessment. Unlike MOTA, HOTA balances precision and recall by decomposing detection, assignment, and localization for a more detailed analysis (Table 1). These metrics gauge how effectively the proposed method tackles key challenges in Multiple Person Tracking (MPT): ID switching, detection failures, occlusion, and handling the appearance/disappearance of individuals. ID switching misassigns identities, detection failures disrupt continuity, and occlusion hides targets. Additionally, newly appearing or disappearing persons may be misidentified, reducing accuracy.

$f_{\theta_{\text{RGB}}}(x_{\text{Full}}^{\text{T}})$  exhibited comparable performance in both Bright and Dark scenes. However, its performance did not reach that of  $f_{\theta_{\text{RGB}}}(x_{\text{Bright}}^{\text{RGB}})$  in the Bright scene.

$f_{\theta_{\text{T}}}(x_{\text{Bright}}^{\text{RGB}})+f_{\theta_{\text{T}}}(x_{\text{Dark}}^{\text{T}})$  achieved comparable performance in both Bright and Dark scenes.

$f_{\theta_{\text{T}}}(x_{\text{Full}}^{\text{T}})$  also demonstrated high performance comparable to  $f_{\theta_{\text{T}}}(x_{\text{Bright}}^{\text{RGB}})+f_{\theta_{\text{T}}}(x_{\text{Dark}}^{\text{T}})$  and, surprisingly, matched the performance of  $f_{\theta_{\text{RGB}}}(x_{\text{Bright}}^{\text{RGB}})$  in the

<sup>1</sup>For this reason, all combinations using the RGB modality in dark scenes are excluded.

<sup>2</sup>For this reason, the performance of  $f_{\theta_{\text{T}}}(x_{\text{Dark}}^{\text{T}})$  is equivalent to that of  $f_{\theta_{\text{T}}}(x_{\text{Bright}}^{\text{T}})$ , and the evaluation of  $f_{\theta_{\text{T}}}(x_{\text{Dark}}^{\text{T}})$  is exempted due to the difficulty in obtaining manual ground-truth annotations.

Table 1. Tracking Accuracy

Tracker	MOTA	IDF1	FP	TP	FN
RGB	38.3	56.3	26	1191	1822
T	93.5	97.0	113	2942	71
FUSION	92.4	96.6	136	2942	71

RGB:  $f_{\theta_{\text{RGB}}}(x_{\text{Dark}}^{\text{T}})$ , T:  $f_{\theta_{\text{T}}}(x_{\text{Dark}}^{\text{T}})$ , FUSION:  $f_{\theta_{\text{RGB}\theta_{\text{T}}}}(x_{\text{Dark}}^{\text{T}}, x_{\text{Dark}}^{\text{T}})$ .

Table 2. Trajectory Prediction Performance

Tracker	HOTA	IDSW
RGB	39.2	12
T	94.1	11
FUSION	93.4	21

Bright scene (Fig. 3). The concern with this method is that it has the drawback of discarding high-resolution information inherent in RGB images.

$f_{\theta_{\text{RGB}}}(x_{\text{Bright}}^{\text{RGB}})+f_{\theta_{\text{RGB}\theta_{\text{T}}}}(x_{\text{Dark}}^{\text{T}})$  achieved slightly inferior results compared to  $f_{\theta_{\text{RGB}}}(x_{\text{Bright}}^{\text{RGB}})+f_{\theta_{\text{T}}}(x_{\text{Dark}}^{\text{T}})$ .

The above suggests that the most effective approach among all the combinations considered here is either switching between two trackers using a simple binary brightness classifier that requires RGB input or reusing the RGB tracker as a pseudo-annotation collector.

Figure 4 visualizes the results of the RGB tracker  $f_{\theta_{\text{RGB}}}$  and the T tracker  $f_{\theta_{\text{T}}}$  on T camera data. The RGB tracker  $f_{\theta_{\text{RGB}}}$  failed to detect many targets, leading to tracking interruptions and false detections. In contrast, the T tracker  $f_{\theta_{\text{T}}}$ , benefiting from knowledge transfer, significantly improved tracking accuracy, reducing missed detections and enhancing ID stability. This is evident from the visually clearer reconstruction of multiple individuals’ boundaries and the effects of occlusion.

## 5 Conclusion

In this study, we tackled the cooperative MPT problem using both RGB and thermal (T) cameras placed in the same pose for the first time. As expected, the RGB tracker completely failed in the Dark scene’s RGB vision and also showed reduced performance in thermal vision. As a solution, we confirmed that learning the T tracker using pseudo-annotations from the RGB tracker is highly effective, achieving the best performance in both Bright and Dark scenes. We also investigated a fusion tracker that integrates both the RGB and T trackers, but surprisingly, its performance ranked second. This suggests that a cooperative approach dynamically switching between the two trackers is more effective than integration. In the future, we aim to apply the developed RGB-T cooperative MPT tracker to real-world robotic vision applications, including recognition, understanding, and reconstruction of individuals, occluders, and traversable areas.

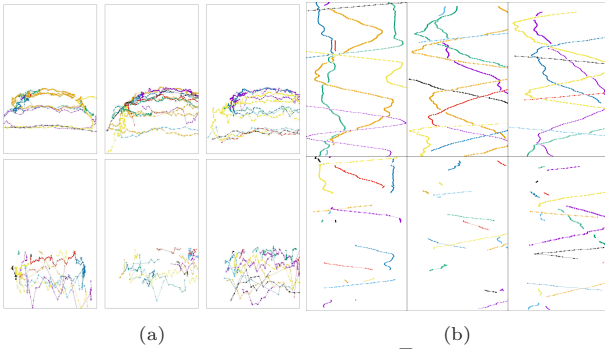


Figure 4. Visualization of  $f_{\theta^T}(x_{\text{Bright}}^T)$  (top) and  $f_{\theta^{\text{RGB}}}(x_{\text{Bright}}^T)$  (bottom). The three-dimensional  $x$ - $y$ - $t$  trajectories are projected onto the  $xy$  plane and  $xt$  plane, shown in panels (a) and (b), respectively. In each panel, the three different columns represent different input image sequences, and different colors indicate different person IDs.

## Acknowledgements

Our work has been supported in part by JSPS KAKENHI Grant-in-Aid for Scientific Research (C) 20K12008 and 23K11270.

## References

- [1] Dean Conte and Tomonari Furukawa. Autonomous robotic escort incorporating motion prediction and human intention. In *2021 IEEE International Conference on Robotics and Automation (ICRA)*, pages 3480–3486. IEEE, 2021.
- [2] Hongliang Guo, Qi Kang, Wei-Yun Yau, Marcelo H. Ang, and Daniela Rus. Em-patroller: Entropy maximized multi-robot patrolling with steady state distribution approximation. *IEEE Robotics and Automation Letters*, 8(9):5712–5719, 2023.
- [3] Berta Bescos, Carlos Campos, Juan D. Tardos, and Jose Neira. Dynaslam ii: Tightly-coupled multi-object tracking and slam. *IEEE Robotics and Automation Letters*, 6(3):5191–5198, 2021.
- [4] Philippe Weinzaepfel, Jerome Revaud, Zaid Harchaoui, and Cordelia Schmid. Learning to detect motion boundaries. In *Proceedings of the IEEE conference on computer vision and pattern recognition*, pages 2578–2586, 2015.
- [5] Panna Felsen, Patrick Lucey, and Sujoy Ganguly. Where will they go? predicting fine-grained adversarial multi-agent motion using conditional variational autoencoders. In *Proceedings of the European conference on computer vision (ECCV)*, pages 732–747, 2018.
- [6] Andreas Doering, Di Chen, Shanshan Zhang, Bernt Schiele, and Juergen Gall. Posetrack21: A dataset for person search, multi-object tracking and multi-person pose tracking. In *Proceedings of the IEEE/CVF Conference on Computer Vision and Pattern Recognition*, pages 20963–20972, 2022.
- [7] Koji Takeda and Kanji Tanaka. Dark reciprocal-rank: Teacher-to-student knowledge transfer from self-localization model to graph-convolutional neural network. In *IEEE International Conference on Robotics and Automation, ICRA 2021, Xi’an, China, May 30 - June 5, 2021*, pages 1846–1853. IEEE, 2021.
- [8] Kanji Tanaka and Eiji Kondo. Vision-based multi-person tracking by using MCMC-PF and RRF in office environments. In *2004 IEEE/RSJ International Conference on Intelligent Robots and Systems, Sendai, Japan, September 28 - October 2, 2004*, pages 637–642. IEEE, 2004.
- [9] Jonathan Tay Yu Liang and Kanji Tanaka. Robot traversability prediction: Towards third-person-view extension of walk2map with photometric and physical constraints. In *IEEE/RSJ International Conference on Intelligent Robots and Systems, IROS 2024, Abu Dhabi, United Arab Emirates, October 14-18, 2024*, pages 11602–11609. IEEE, 2024.
- [10] Jiajun Jiang, Xingxin Chen, Weichen Dai, Zelin Gao, and Yu Zhang. Thermal-inertial slam for the environments with challenging illumination. *IEEE Robotics and Automation Letters*, 7(4):8767–8774, 2022.
- [11] Jialian Li, Jingyi Zhang, Zhiyong Wang, Siqi Shen, Chenglu Wen, Yuexin Ma, Lan Xu, Jingyi Yu, and Cheng Wang. Lidarcap: Long-range marker-less 3d human motion capture with lidar point clouds. In *Proceedings of the IEEE/CVF conference on computer vision and pattern recognition*, pages 20502–20512, 2022.
- [12] Jonathon Luiten, Tobias Fischer, and Bastian Leibe. Track to reconstruct and reconstruct to track. *IEEE Robotics and Automation Letters*, 5(2):1803–1810, 2020.
- [13] Kruttidipta Samal, Hemant Kumawat, Priyabrata Saha, Marilyn Wolf, and Saibal Mukhopadhyay. Task-driven rgb-lidar fusion for object tracking in resource-efficient autonomous system. *IEEE Transactions on Intelligent Vehicles*, 7(1):102–112, 2021.
- [14] Zhi Yan, Li Sun, Tom Duckett, and Nicola Bellotto. Multisensor online transfer learning for 3d lidar-based human detection with a mobile robot. In *2018 IEEE/RSJ International Conference on Intelligent Robots and Systems (IROS)*, pages 7635–7640. IEEE, 2018.
- [15] Zongwei Wu, Jilai Zheng, Xiangxuan Ren, Florin-Alexandru Vasluianu, Chao Ma, Danda Pani Paudel, Luc Van Gool, and Radu Timofte. Single-model and any-modality for video object tracking. In *Proceedings of the IEEE/CVF conference on computer vision and pattern recognition*, pages 19156–19166, 2024.
- [16] Ciarán Ó Conaire, Noel E. O’Connor, and Alan F. Smeaton. Thermo-visual feature fusion for object tracking using multiple spatiogram trackers. *Mach. Vis. Appl.*, 19(5-6):483–494, 2008.
- [17] Stan Birchfield and Sriram Rangarajan. Spatiograms versus histograms for region-based tracking. In *2005 IEEE Computer Society Conference on Computer Vision and Pattern Recognition (CVPR 2005), 20-26 June 2005, San Diego, CA, USA*, pages 1158–1163. IEEE Computer Society, 2005.

- [18] Yi Wu, Erik Blasch, Genshe Chen, Li Bai, and Haibin Ling. Multiple source data fusion via sparse representation for robust visual tracking. In *Proceedings of the 14th International Conference on Information Fusion, FUSION 2011, Chicago, Illinois, USA, July 5-8, 2011*, pages 1–8. IEEE, 2011.
- [19] Huaping Liu and Fuchun Sun. Fusion tracking in color and infrared images using joint sparse representation. *Sci. China Inf. Sci.*, 55(3):590–599, 2012.
- [20] Chenglong Li, Hui Cheng, Shiyi Hu, Xiaobai Liu, Jin Tang, and Liang Lin. Learning collaborative sparse representation for grayscale-thermal tracking. *IEEE Trans. Image Process.*, 25(12):5743–5756, 2016.
- [21] Chenglong Li, Xiang Sun, Xiao Wang, Lei Zhang, and Jin Tang. Grayscale-thermal object tracking via multitask laplacian sparse representation. *IEEE Trans. Syst. Man Cybern. Syst.*, 47(4):673–681, 2017.
- [22] Chenglong Li, Chengli Zhu, Yan Huang, Jin Tang, and Liang Wang. Cross-modal ranking with soft consistency and noisy labels for robust RGB-T tracking. In Vittorio Ferrari, Martial Hebert, Cristian Sminchisescu, and Yair Weiss, editors, *Computer Vision - ECCV 2018 - 15th European Conference, Munich, Germany, September 8-14, 2018, Proceedings, Part XIII*, volume 11217 of *Lecture Notes in Computer Science*, pages 831–847. Springer, 2018.
- [23] Chenglong Li, Nan Zhao, Yijuan Lu, Chengli Zhu, and Jin Tang. Weighted sparse representation regularized graph learning for RGB-T object tracking. In Qiong Liu, Rainer Lienhart, Haohong Wang, Sheng-Wei "Kuan-Ta" Chen, Susanne Boll, Yi-Ping Phoebe Chen, Gerald Friedland, Jia Li, and Shuicheng Yan, editors, *Proceedings of the 2017 ACM on Multimedia Conference, MM 2017, Mountain View, CA, USA, October 23-27, 2017*, pages 1856–1864. ACM, 2017.
- [24] Chenglong Li, Xinyan Liang, Yijuan Lu, Nan Zhao, and Jin Tang. RGB-T object tracking: Benchmark and baseline. *Pattern Recognit.*, 96, 2019.
- [25] Goutam Bhat, Martin Danelljan, Luc Van Gool, and Radu Timofte. Learning discriminative model prediction for tracking. In *2019 IEEE/CVF International Conference on Computer Vision (ICCV)*, pages 6181–6190, 2019.
- [26] Lichao Zhang, Martin Danelljan, Abel Gonzalez-Garcia, Joost van de Weijer, and Fahad Shahbaz Khan. Multi-modal fusion for end-to-end RGB-T tracking. *CoRR*, abs/1908.11714, 2019.
- [27] Yifu Zhang, Peize Sun, Yi Jiang, Dongdong Yu, Fucheng Weng, Zehuan Yuan, Ping Luo, Wenyu Liu, and Xinggang Wang. Bytetrack: Multi-object tracking by associating every detection box. In *European conference on computer vision*, pages 1–21. Springer, 2022.
- [28] Jinkun Cao, Jiangmiao Pang, Xinshuo Weng, Rawal Khirodkar, and Kris Kitani. Observation-centric SORT: rethinking SORT for robust multi-object tracking. In *IEEE/CVF Conference on Computer Vision and Pattern Recognition, CVPR 2023, Vancouver, BC, Canada, June 17-24, 2023*, pages 9686–9696. IEEE, 2023.
- [29] Yunhao Du, Zhicheng Zhao, Yang Song, Yanyun Zhao, Fei Su, Tao Gong, and Hongying Meng. Strongsort: Make deepsort great again. *IEEE Trans. Multim.*, 25:8725–8737, 2023.
- [30] Anton Milan, Laura Leal-Taixé, Ian Reid, Stefan Roth, and Konrad Schindler. Mot16: A benchmark for multi-object tracking. *arXiv preprint arXiv:1603.00831*, 2016.
- [31] Patrick Dendorfer, Hamid Rezaatofighi, Anton Milan, Javen Shi, Daniel Cremers, Ian Reid, Stefan Roth, Konrad Schindler, and Laura Leal-Taixé. Mot20: A benchmark for multi object tracking in crowded scenes. *arXiv preprint arXiv:2003.09003*, 2020.
- [32] Shuai Shao, Zijian Zhao, Boxun Li, Tete Xiao, Gang Yu, Xiangyu Zhang, and Jian Sun. Crowdhuman: A benchmark for detecting human in a crowd. *arXiv preprint arXiv:1805.00123*, 2018.
- [33] Shanshan Zhang, Rodrigo Benenson, and Bernt Schiele. Citypersons: A diverse dataset for pedestrian detection. In *Proceedings of the IEEE conference on computer vision and pattern recognition*, pages 3213–3221, 2017.
- [34] Andreas Ess, Bastian Leibe, Konrad Schindler, and Luc Van Gool. A mobile vision system for robust multi-person tracking. In *2008 IEEE conference on computer vision and pattern recognition*, pages 1–8. IEEE, 2008.
- [35] Jonathon Luiten, Aljosa Osep, Patrick Dendorfer, Philip Torr, Andreas Geiger, Laura Leal-Taixé, and Bastian Leibe. Hota: A higher order metric for evaluating multi-object tracking. *International journal of computer vision*, 129:548–578, 2021.